



Thermodynamic calculations of a two-phase thermosyphon loop for cold neutron sources



Victor-O. de Haan^{a,*}, René Gommers^b, J. Michael Rowe^c

^a *BonPhysics Research and Investigations BV, Laan van Heemstede 38, 3297AJ Puttershoek, The Netherlands*

^b *Reactor Institute Delft, Delft University of Technology, Mekelweg 15, 2629JB Delft, The Netherlands*

^c *Department of Materials Science and Eng., University of Maryland, NIST Center for Neutron Research, National Institute of Standards and Technology, Gaithersburg, MD 20899-8562, United States*

ARTICLE INFO

Article history:

Received 20 January 2017

Received in revised form 23 May 2017

Accepted 24 May 2017

Available online 27 May 2017

Keywords:

Thermosyphon loop
Two-phase flow
Numerical modeling
Hydrogen
Deuterium
Void fraction

ABSTRACT

A new method is described for thermodynamic calculations of a two-phase thermosyphon loop based on a one-dimensional finite element division, where each time-step is split up in a change of enthalpy and a change in entropy. The method enables the investigation of process responses for a cooling loop from room temperature down to cryogenic temperatures. The method is applied for the simulation of two distinct thermosyphon loops: a two-phase deuterium and a two-phase hydrogen thermosyphon loop. The simulated process responses are compared to measurements on these loops. The comparisons show that the method can be used to optimize the design of such loops with respect to performance and resulting void fractions.

© 2017 Elsevier Ltd. All rights reserved.

1. Introduction

A good understanding of two-phase thermosyphon loops is crucial for further development and optimization of efficient cryogenic cooling loops. Specifically for the development of efficient moderators for cold neutrons it is of paramount importance to understand the thermosyphon loop and its dynamic characteristics.

Although the development of cold neutron sources already started in the 1970's, the current development of stronger neutron sources (for instance at the European Spallation Source [1]) calls for the investigation of the efficiency of the cooling design. Also, as in case of the OYSTER project of the Delft University of Technology [2], if optimization of the performance of both neutron moderation and cooling efficiency is needed, a detailed knowledge of the cooling process involved is required. In case of a two-phase thermosyphon loop, the void fraction inside the moderator cell is a critical factor for efficient moderation of neutrons. For a two-phase flow, the void consists of gaseous moderator (for instance hydrogen or deuterium vapor) which has a much smaller density than the liquid part. However, for optimal moderation, density is

a critical parameter and hence the actual void fraction in the moderator cell determines the performance of the neutron source.

A numerical model is created to study trends in the dynamics of the thermosyphon loop. The model is based on a linear finite element division of the loop where each element has certain characteristics. The model is solved using the principles of conservation of mass, energy and momentum.

Similar models have been constructed in literature by for instance Dobson [3,4], Kaya [5], Bielinski [6] and Zhang [7]. The main difference here is the way that the flow dynamics are incorporated. Basically, it comes down to acknowledging the fact that *temperature changes due to (changing) heat flows are in general much slower than pressure changes due to changing mass flows*. Hence, the acceleration term of the flowing mass is ignored and a steady flow state is assumed at every time step. This is known as the *quasi-static motion approximation*. The mass flow in and out an element is the same. However, if this is strictly followed the mass in the element cannot change. To mitigate this, it is assumed that mass transport from one element to another is adiabatic, where the total entropy of the mass is constant.

2. System description

The moderator cell and its content are cooled by means of a shell and tube heat exchanger. The moderating material itself is

* Corresponding author.

E-mail address: victor@bonphysics.nl (V.-O. de Haan).

used to transport the heat load from the moderator cell towards the heat exchanger. The transport is provided by the thermosyphon principle as shown in Fig. 1. The heat load is due to the nuclear gamma and fast neutron radiation accompanying the cold neutron radiation. Also, thermal and cold neutron capture in both moderator and moderator cell wall contribute to the heat load.

The thermosyphon is a loop containing an evaporator (moderator cell), a condenser (heat exchanger) and a buffer volume. The driving force for the mass transport is gravity-based and therefore fail-safe. A buffer volume is connected to the loop for inventory control and storage during the hot or non-operating mode of the loop. The gaseous moderator rising in the riser is condensed in the tubes of the heat exchanger by means of film condensation. The condensation heat is removed by sufficient helium flow. The condensate is not sufficient to block the condensing tubes inner diameter, hence the gas pressure in heat exchanger is almost a static pressure. Further, the diameter of the downcomer should be sufficiently large to let a liquid film drop into the moderator cell. In the downcomer the film is changed into a complete filled tube, from which point the pressures starts to increase due to the weight of the liquid column. Then, there is also some slight sub-cooling of the liquid. In the moderator cell the liquid is evaporated, taking up the heat load. The vapor bubbles accelerate (almost without friction) to the top of the moderator cell where they merge and enter the riser. The vapor is then raised to the top of the heat exchanger, where the loop restarts. The pressure drop during the transport through the riser is compensated by the pressure provided by the weight of the liquid column.

Under static conditions, the complete heat load provided to the moderator cell (and other parts) is transported to the heat-exchanger and removed by the helium. Under dynamic conditions the temperature of all parts change in time and the temperature dependent heat capacity of all items must be taken into account.

It is essential to treat the moderator cell differently from the supply and return lines: it is closer to pool boiling than to normal two-phase flow in pipes. This is treated in A. A similar argument holds for the tube side of the heat exchanger. This is much closer to plate condensing than to normal two-phase flow. This is treated in B.

Simulations of thermosyphon loops have been performed by for instance Dobson [3,4], Bielinski [6] and Zhang [7]. However in these cases a limited temperature range has been applied where the loop is either always single-phase or two-phases. Here we need

the behavior between room temperature and cryogenic temperature so that the transition from 1 phase into 2 phases and vice versa should be considered. This is implemented by an appropriate form of the conservation laws.

3. Method

The method is based on the use of a 1D finite element method as used previously by Dobson [4]. All the parts of the thermosyphon loop (see Fig. 1, left side) are coded by means of 1 or more elements that are connected to one, two or three other elements depending on the function of the part. For instance, the riser connecting the moderator cell with the heat exchangers is modeled by 15 elements. The first element of the riser is connected to the moderator element and the last element is connected to the heat exchanger. In this way a loop of elements is constructed from heat exchanger via the downcomer to the moderator cell and via the riser back to the heat exchanger. The mass flow in this loop is everywhere the same. In a similar way another series of elements is constructed between the buffer and the heat exchanger where the mass flow is also constant, although different from the mass flow in the loop (see Fig. 1, right side). The same is done for the parts of the helium loop. The loops are connected at the heat exchanger, where the heat load of the heat exchanger of the thermosyphon loop equals the heat sink of the heat exchanger of the helium loop.

The mass flow through the elements results in a pressure drop because of the friction with the wall. The momentum pressure drop due to evaporation or condensation is neglected (see Appendix F). For constant mass flows, starting from the pressure in the buffer, all pressures in the elements are fixed. The simulation is performed by defining a time step and determining for each element the heat load or sink during that time step. This heat load or sink changes the enthalpy of the contents resulting in a changed pressure and temperature in an element. This change in pressure and temperature give rise to a change in mass in the element that is calculated by means of the concept of adiabatic mass transport resulting in pressure and mass flow changes. After the new masses and pressures have been calculated the next time step is applied.

3.1. Definition of an element

An element is defined as a container interacting with the environment and the material inside the container with 1–3 inputs

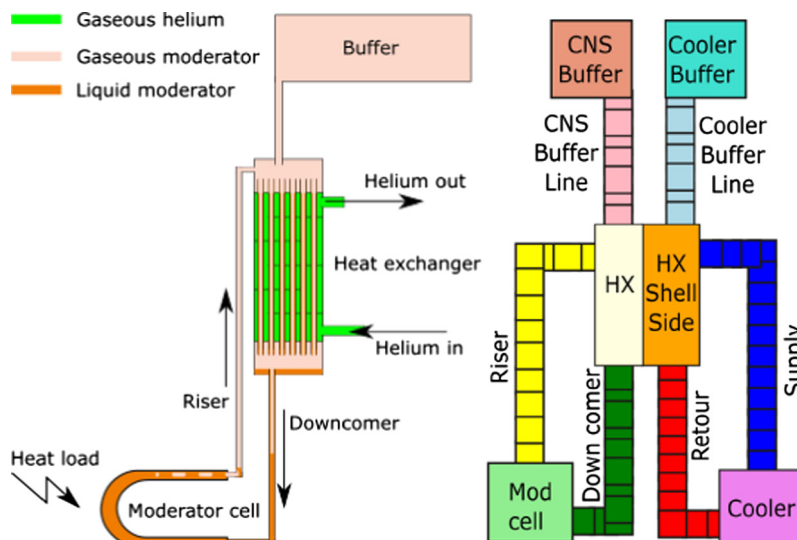


Fig. 1. Thermosyphon loop (left) divided in linear elements (right).

and/or outputs. An element with 1 input/output is used to simulate the buffer. An element with 3 inputs/outputs is used to simulate the part of the thermosyphon loop where the buffer is connected, here the heat exchanger.

The gas and/or liquid interacts via the inputs and outputs with the other elements. The interaction is based on three conservation laws: i.e. mass, energy and momentum, and the assumption of *quasi-static motion*. This means that the acceleration of the flow is assumed to be zero and the rate at which pressure waves are propagated through the material is much higher than the rate at which mass and heat moves in the loop. This assumption is allowed as the velocity of the material is much less than the velocity of sound. Hence it is safe to assume a quasi-static solution for the equation of motion, so that Bernoulli's law (the sum of static pressure, dynamic pressure and gravitational pressure is constant) and the gas law for gasses (pressure as a function of temperature and density) can be applied. Hence, it is assumed the dynamical effects are due only to the temperature changes in the system and the heat transfer.

Each input/output of an element is connected to 1 input/output of another element, and at the connections the mass flows and pressures are equal.

3.2. Definition of a container

The energy flows towards and inside the container are shown in Fig. 2. The container exchanges heat with the environment due to a temperature difference. The heat flow from or to the environment is divided into two parts: the heat flow due to conduction and the one due to thermal radiation. The conduction heat is proportional to the temperature difference between container wall and environment, hence

$$Q^C = A_c h_e (T_e - T_o) \quad (1)$$

where T_o is the outside temperature of the container wall, T_e is the environmental temperature, A_c is the effective area of the container and h_e is the heat transfer coefficient of the container to the environment. It is determined by the heat transfer coefficients between wall and environment and the effective areas involved. It might be temperature dependent. The radiation heat flow is proportional to the 4th power of the temperatures according to

$$Q^R = A_c \epsilon_c \sigma_B (T_e^4 - T_o^4) \quad (2)$$

where $\sigma_B = 5.67 \times 10^{-8} \text{ W}/(\text{m}^2 \text{ K}^4)$ is Stephan-Boltzmanns constant and ϵ_c is the emissivity coefficient. When super insulation is applied this might be different as this reduces radiation by a factor of two per layer. Here this is incorporated by reducing the emissivity coefficient. The conduction heat flow from the outside to the inside of the container wall is determined by

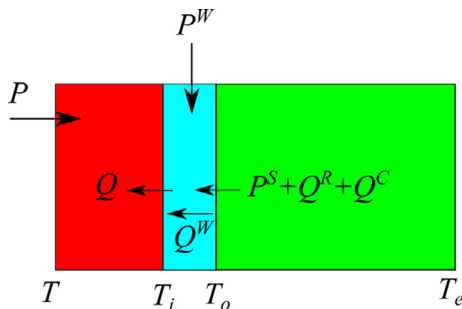


Fig. 2. Overview of energy flows in container wall. From left to right: container (red), wall (blue) and environment (green). (For interpretation of the references to colour in this figure legend, the reader is referred to the web version of this article.)

$$Q^W = A_c \frac{\lambda_c}{d_c} (T_o - T_i) \quad (3)$$

where λ_c is the thermal conductivity of the wall material, and d_c the thickness of the container wall. It might also be temperature dependent. Furthermore, the container can be subjected to an additional heat load (or sink) at the surface of the container, denoted by P^S . Lastly the nuclear radiation heat load is taken into account by the container wall heat load density P^W and moderator heat load density P both expressed in W/kg. They can be calculated by multiplying the specific nuclear radiation heat load (i.e. the nuclear heat load per kg material experienced due to a reactor power of 1 MW) by the nuclear power of the reactor, P^N expressed in MW. The temperature of the container varies depending on the applied loads, mass flow and material of the container. The way this is taken into account is addressed in Appendix C and Appendix D.

The container of each element contains gas and/or liquid. The temperature difference between the inside container wall and the gas and/or liquid results in heat transport between the container wall and the contents according to

$$Q = A_c h_c (T_i - T) \quad (4)$$

where h_c is the heat transfer coefficient between wall and contents. This coefficient depends on the phase and the kind of flow. Here, for an assumed homogeneous flow inside a circular pipe, it is approximated by using the Dittus-Boelter relation (as introduced by McAdams [8]) between the Nusselt number, the Reynolds number and the Prandtl number

$$Nu = 0.023 Re^{0.8} Pr^{0.4} \quad (5)$$

where Reynolds number is given by

$$Re = \frac{\rho v D}{\eta} = \frac{4 \Phi}{\pi \eta D} \quad (6)$$

where ρ is the density, v is the velocity, η is the dynamic viscosity and D the effective diameter of the pipe cross section and Φ is the mass flow. The Prandtl number is given by

$$Pr = \frac{C_p \eta}{\lambda} \quad (7)$$

and is a material property depending on temperature. C_p is the heat capacity of the gas or liquid and λ its thermal conductivity. From the definition of Nusselt number

$$h_c = \frac{\lambda Nu}{D} \quad (8)$$

An exception for this is the heat transfer coefficient in the heat exchangers where the gas condenses on the wall into a thin film which starts flowing down. The way the heat transfer coefficient is calculated is explained in Appendix B.

3.3. Definition of an input/output

Each input/output is characterized by 5 parameters:

Gravitational height. As gravitation is the driving force for the thermosyphon loop, each input/output is characterized by a specific height defining the height difference between the input/output and the center of mass of the element. This is referred to as gravitational height. The pressure difference due to the gravitational height between the input and output of an element must be compensated by a difference in pressure between two consecutive elements or an internal resistance so that the resulting flow is stationary in order to conform to the principle of the quasi-static solution.

Liquid and Gaseous mass flow. As a two phase flow is considered, both the liquid and gaseous (or vapor) flow at each input should be

defined. In such a case the total mass flow and total enthalpy flow is known.

Pressure at input/output. The pressure of the liquid and gas are assumed to be identical at any point in the loop. This corresponds to the quasi-static motion approximation. The pressure at an input/output of an element will be set equal to the pressure at an input/output of a connected element.

Friction coefficient The friction coefficient defines the relation between the pressure drop in an element from one input/output to another one and the mass flowing between these parts. In general it is dependent on the density of the material and the type of flow. Here three possibilities are considered. Pure vapor flow, pure liquid flow and two-phase flow. The way the pressure drop (i.e. the effective friction coefficient) is calculated is explained in Appendix F.

3.4. Material properties

For the calculations the material properties over the relevant temperature range are needed. For the container wall two materials are considered: aluminum and stainless steel.

Hydrogen properties are taken from the equation of state published by Leachman [9] for normal hydrogen. Hydrogen molecules can have two different energy states, depending on the mutual spin direction of the constituting atoms. For ortho-hydrogen the spins are parallel, for para-hydrogen the spins are anti-parallel. Normal hydrogen is hydrogen for which the ortho- and para-hydrogen molecules are in thermal equilibrium. In the calculations, the differences in material properties due to the transitions between ortho and para hydrogen are ignored. Using the equation of state the enthalpy, entropy and pressure can be calculated as function of temperature and density. The density for the vapor and liquid is calculated as a function of the saturation pressure at a certain temperature. The thermal conductivity of hydrogen is taken from Assael [10] and its dynamic viscosity from Muzny [11].

Deuterium properties are taken from the equation of state published by Richardson [12] for normal deuterium. The differences in material properties due to the transitions between ortho and para deuterium are ignored. The thermal conductivity and dynamic viscosity of deuterium are taken from the NIST Standard Reference Database [13]. Helium properties are taken from Bell [14]. For aluminum the properties of alloy Al6061 are used and for stainless steel the properties of alloy SS304 as published by Duthil [15].

3.5. Iterations

The dynamic behavior is calculated by iterative time step. The iteration steps are schematically shown in Fig. 3.

During the time between each time step j (from time t_j to t_{j+1}) it is assumed that all time-derivatives are constant, like mass flow and heat flow. For each element k the conservation laws are applied to determine the starting values for the next time step. **Conservation of mass.** The total mass in the loop is constant, hence the total mass flowing in or out an element (liquid mass flow $\Phi_{i,k,j}^L$ and gaseous mass flow $\Phi_{i,k,j}^V$) is equal to the mass accumulation or reduction

$$\forall_k \left\{ \sum_{i=1}^{n_k} (\Phi_{i,k,j}^L + \Phi_{i,k,j}^V) (t_{j+1} - t_j) = m_{k,j+1}^L + m_{k,j+1}^V - m_{k,j}^L - m_{k,j}^V \right\} \quad (9)$$

where k ranges over all elements, i over all inputs/outputs and j is the time step considered.

Conservation of energy. The change of energy in the content mass is equal to the energy gain/loss from/towards the wall or by the flow of mass, hence

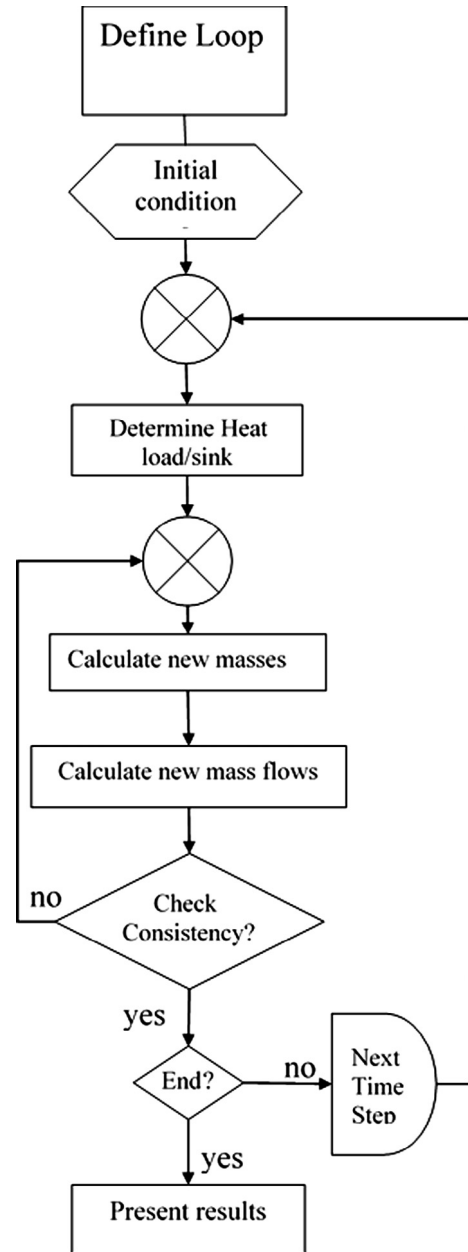


Fig. 3. Calculation scheme of thermosyphon loop.

$$\forall_k \left\{ \begin{aligned} & (P_{k,j}(m_{k,j}^L + m_{k,j}^V) + Q_{k,j})(t_{j+1} - t_j) + \\ & \sum_{i=1}^{n_k} (\Phi_{i,k,j}^L H_{i,k,j}^L + \Phi_{i,k,j}^V H_{i,k,j}^V) (t_{j+1} - t_j) = \\ & m_{k,j+1}^L H_{k,j+1}^L + m_{k,j+1}^V H_{k,j+1}^V - m_{k,j}^L H_{k,j}^L - m_{k,j}^V H_{k,j}^V \end{aligned} \right\} \quad (10)$$

where $H_{i,k,j}^L$ is the enthalpy of the liquid at element k and time step j if $\Phi_{i,k,j}^L < 0$ and otherwise $H_{i,k,j}^L$ is the enthalpy of the liquid at the element connected to input/output i . It is determined by the local density and temperature of the liquid. $H_{i,k,j}^V$ is the enthalpy of vapor (or gas) at element k and time step j if $\Phi_{i,k,j}^V < 0$ and otherwise $H_{i,k,j}^V$ is the enthalpy of the vapor at the element connected to input/output i . It is determined by the local density and temperature of the vapor (or gas).

The change of energy of the container wall is equal to the energy gain/loss from/towards the environment, hence

$$\forall_k \left\{ \sum_{i=1}^{n_k} (p_{k,j}^W + Q_{k,j}^S - Q_{k,j}) (t_{j+1} - t_j) = m_k^C (H_{k,j+1}^C - H_{k,j}^C) \right\}. \quad (11)$$

where $H_{k,j}^C$ is the enthalpy of container material at element k and time step j . It is determined by the local density and temperature of the container. $Q^S = P^S + Q^R + Q^C$ is the energy flow from the environment to the container wall.

Conservation of momentum. The conservation of momentum in the loop is used to determine the pressure changes in the loop. The pressure difference between element and input/output of an element is given by

$$\forall_{k,i} \left\{ (p_{k,j}^i - (p_{k,j} - \rho_{k,j} g \Delta h_{i,k})) = f_{i,k,j} \frac{\Delta L_{i,k}}{DA_C^2} \frac{\Phi_{i,k,j}^2}{2\rho_{k,j}} \right\} \quad (12)$$

where g is the gravitation constant and $\Delta L_{i,k}$ is the effective length of the input/output to the element. The effective friction factors $f_{i,k,j}$, mass flows $\Phi_{i,k,j}$ and densities $\rho_{k,j}$ are calculated according to the method described in Appendix F.

Each input/output of an element k, i is connected to 1 input/output of another element k, i , at the connection the mass flows and pressures are equal:

$$\begin{aligned} p_{k,j}^i &= p_{k',j}^i \\ \Phi_{i,k,j}^L &= \Phi_{i',k',j}^L \\ \Phi_{i,k,j}^V &= \Phi_{i',k',j}^V \end{aligned} \quad (13)$$

Initial state. Initially the loop is filled with a certain amount of gas at room temperature. All the mass flows are zero and the loop is in pressure equilibrium including the difference in hydrostatic pressure. All heat loads/sinks are initially zero and to start the calculation, a change in heat load or heat sink is applied at some element(s) of the loop.

The first calculation step is to determine the quantity of these heat loads (or heat sinks) that might depend on the density, temperature or dimensions of the materials in the loop.

The second step is to determine the container wall and contents response to this heat load. The container wall can be calculated by

means of Eq. (11). Details of the calculation can be found in Appendix C. The contents response might be translated into a pressure and temperature transient or into evaporation or condensation changing the void fraction of the element. This depends on the state of the content in the element and the interaction with the container wall. By means of Eqs. (9) and (10) it is possible to calculate the values of the pressure and temperature of the liquid and vapor (or gas) mass. Details of these calculations are described in Appendix D. Finally, the mass distribution at the end of the step is calculated. As argued the quasi-static motion approximation is used so there is no net mass flow in or out an element. However, if this is strictly followed, unnatural behavior occurs as the masses in the element could not change. Hence, it is assumed that adiabatic mass transport occurs where the total entropy of the mass will remain constant. This is described in Appendix E.

The third step is to calculate the flow conditions due to the content state in each element by using Eqs. (12) and (13).

It should be noted that for Eq. (10) also the enthalpy at the end of the time step is needed. The enthalpy depends on the pressure and temperature that will change between steps. Hence, the above steps 2 and 3 need to be repeated until no relevant changes occur. If this procedure does not converge, the time step must be reduced until it does.

4. Simulations and results

As an example two thermosyphon loops are considered. The first example is the thermosyphon loop used to cool down a hydrogen moderator at NIST. The second example is from a publication in which a deuterium thermosyphon loop is described.

4.1. Example 1

NIST PeeWee [16] hydrogen cold neutron source is simulated. The thermosyphon loop of PeeWee, as shown in Fig. 4, is cooled by means of a plate-and-fin heat exchanger. This was simulated by a tube-and-shell heat exchanger with similar thermal transport properties and pressure drop values. The design data used for the

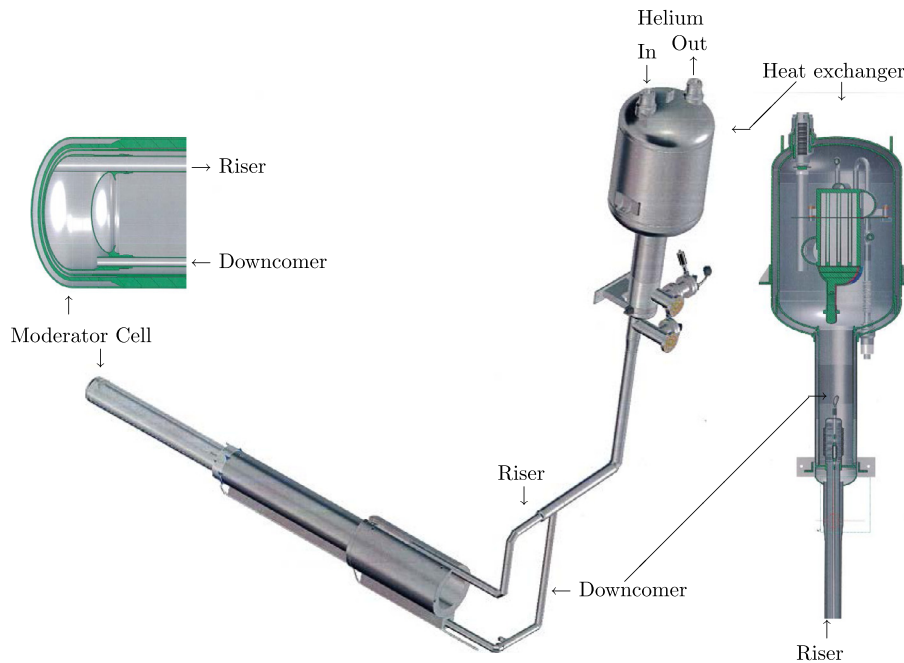


Fig. 4. NIST PeeWee hydrogen cold neutron source thermosyphon loop.

Table 1
Design data PeeWee hydrogen loop.

Name	Buffer	Line	Riser	HX	Down comer	Cell	Unit
Material	SS304	SS304	Al6061	Al6061	Al6061	Al6061	–
ϵ_c	0.1	0.1	0.1	0.1	0.1	0.1	–
h_e	1000	1	0.001	0.001	0.001	0.1	W/m ² /K
d_w	10	2	0.78	6.6	0.78	1.38	mm
T_e	300	300	300	300	300	300	K
P/P^N	0	0	0	0	0	40	ppm/kg
P^W/P^N	0	0	0	0	0	110	ppm/kg
D	20	22	14	20	20	7.75	mm
ϵ	10	10	1	1	1	1	ppm
ΔH	0	2.5	–2.43	0.27	2.255	–0.09455	m
ΔL	1	16.9	5.39	0.27	6.058	0.11	m
A_C	1					0.041	m ²
V_C	0.5					0.000436	m ³
V_O				0.15		0	dm ³
σ_O				0.1		2	

Table 2
Design data PeeWee helium Loop.

Name	Buffer	Line	Supply	HX	Retour	Cooler	Unit
Material	SS304	SS304	SS304	Al6061	SS304	Al6061	–
ϵ_c	0.1	0.1	0.05	0.1	0.05	0.1	–
h_e	1000	1	0.001	0.001	0.001	0.001	W/m ² /K
d_w	0.01	0.002	0.002	0.002	0.002	0.002	m
T_e	300	300	300	300	300	300	K
D	0.02	0.0355	0.06	0.0062	0.04	0.01	m
ϵ	10	10	10	10	10	10	ppm
ΔH	0	5	–0.27	0.27	0	0	m
ΔL	1	10	27	0.27	27	0.5	m
A_C	1					1	m ²
V_C	0.92					0.15	m ³

Table 3
Volumes and masses PeeWee Loops.

Name	Volume dm ³	Area m ²	Content Mass gram	Empty mass kg
Moderator Cell	0.436	0.041	8.31	0.453
Heat exchanger	6.09	5.7	82.6	14.58
CNSBuffer	500	1	81.3	80
Cold CNS Loop	7.65	6.13	125	15.6
Total CNS Loop	514.1	8.30	207	114
Cooler	150	1	1426	5.43
HXShellSide	3	2.52	21.4	0.68
CoolerBuffer	920	1	490	80
Cold Cooler Loop	263.3	12.01	2356	142
Total Cooler Loop	1293	14.12	2852	240

hydrogen loop is shown in Table 1. The helium loop is approximated and has been designed to give results corresponding to the refrigerator of the helium loop of PeeWee. The design data used for the helium loop is shown in Table 2. Both loops are cooled down starting from environmental temperature (300 K). The hydrogen loop starting pressure is 500 kPa, the helium loop starting pressure is 1500 kPa. The resulting volumes and masses after cooling down to approximately 23 K are shown in Table 3. The pressure in the hydrogen loop reduced to approximately 200 kPa.

The cool down curves shown in the left side of Fig. 5 are typical measured values as obtained by NIST and the ones to the right side are calculated by means of the method described above. Although an accurate match has not been obtained, one can conclude that time constants are of the same order of magnitude. It should be noted that the helium loop is approximated and hence the cool down of the helium is at best a rough estimate. As soon as the hydrogen loop starts to flow the simulated temperature changes are more comparable to the actual ones.

The temperature difference over the helium side of the heat exchanger during cool down behaves similar and is of the same order of magnitude. The temperature of the hydrogen riser close to the heat exchanger behaves in a similar manner, but the temperature in the downcomer close to the heat exchanger behaves differently (the peak at the moment the hydrogen condenses is not reproduced). This is probably due to thermal conduction effects in the wall material along the flow direction that are not taken into account in the simulation. These are especially important as long as the hydrogen flow is very small.

The pressure change in the hydrogen loop behaves similarly. First a gradual decrease until the hydrogen starts to flow and the thermosyphon starts its operation in a single (gas) phase. Then, a rise in pressure occurs because the hydrogen is heated by the parts of the loop that are still warm. After sufficient time has passed, the loop has cooled down sufficiently so that the hydrogen that enters the heat exchanger is condensed and the single-phase thermosyphon starts to change in a two-phase thermosyphon. This

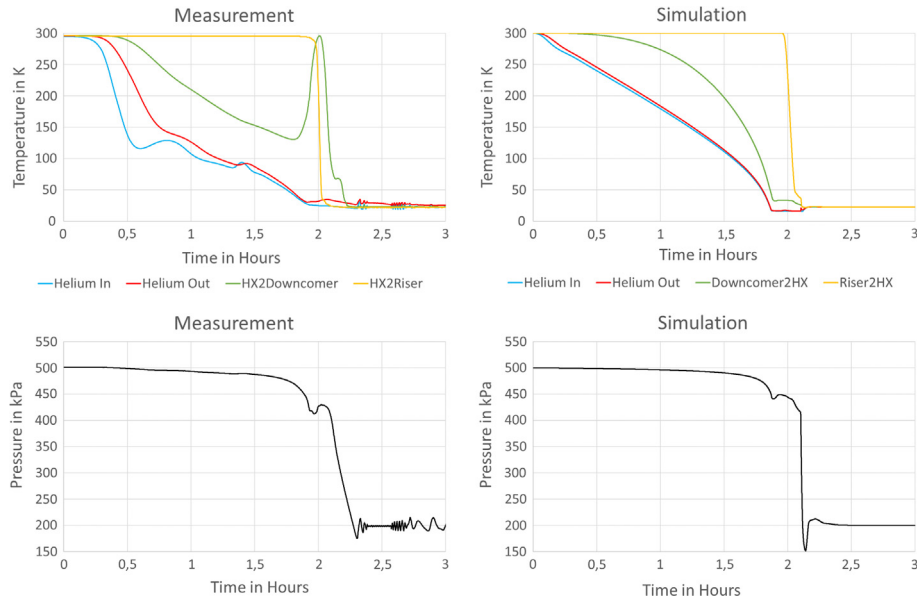


Fig. 5. Cool down curves. Left side: Typical measured values as obtained by NIST. Right side: Values obtained from simulation. Top: Temperature at several locations in helium and hydrogen loop. Bottom: Hydrogen pressure as function of time during cool down.

Table 4
Design data ILL Deuterium Mockup Loop.

Name	Buffer	Line	Riser	HX	Down comer	Cell	Unit
Material	SS304	SS304	Al6061	Al6061	Al6061	Al6061	–
ϵ_c	0.1	0.1	0.1	0.1	0.1	0.1	–
h_c	1000	1	0.001	0.001	0.001	0.1	W/m ² /K
d_w	10	2	1	6.6	1	1	mm
T_e	300	300	300	300	300	300	K
P/P^N	0	0	0	0	0	60	ppm/kg
P^W/P^N	0	0	0	0	0	165	ppm/kg
D	20	22	24	20	20	15.4	mm
ϵ	10	10	1	1	1	1	ppm
ΔH	0	2.5	–4.25	1	3.45	–0.2	m
ΔL	1	16.9	8	1	8.41	0.3	m
A_c	8					0.132	m ²
V_c	4					0.007	m ³
V_o				1		0.0045	dm ³
σ_o				1		1	

increases the effective heat transfer coefficient of the heat exchanger and the cooling down is accelerated and the pressure decreases again until the pressure control regulates the pressure to 200 kPa.

4.2. Example 2

The ILL deuterium Mockup loop as described by Hoffmann [17] is simulated. The thermosyphon loop is cooled by means of a heat exchanger, simulated as a tube-and-shell heat exchanger. The right side of Fig. 1 is a schematic diagram of the loops and the names of the parts. The design data used for the deuterium loop is shown in Table 4. The helium loop is approximated and has been designed to give results corresponding to the refrigerator of the helium loop of the ILL mockup. The design data used for the helium loop is shown in Table 5. Both loops are cooled down starting from environmental temperature (300 K). The deuterium loop starting pressure is 500 kPa, the helium loop starting pressure is 1500 kPa. The resulting volumes and masses after cooling down the loops to a temperature of roughly 25.2 K are shown in Table 6. The pressure in the deuterium loop reduced to approximately 150 kPa.

The flow resistance of the moderator cell was approximately matched to the measurements and the overflow volume of the moderator cell was approximately matched to get a corresponding

void fraction of the moderator cell. The pressure drop due to the flow resistance in the loop is shown in Fig. 6. The background of the figure is taken from Hoffmann [17] so that simulated data can directly be compared to the measurements reported. The black dots and hatched areas represent the measurements and estimated accuracy region of pressure drops in the loop. The black lines represent calculations as presented by Hoffmann. The colored lines represent the same pressure drops calculated using the simulations as presented here.

The simulations and measurements give the same general trends. With increasing heating power the mass flow increases because the amount of void fraction that needs to be transported from moderator cell to heat exchanger increases. With increasing mass flow the pressure drop increases. The pressure drop for the single-phase flow (downcomer) reaches a maximum and then reduces again. This maximum is obtained at the maximum mass flow (right side of Fig. 6). The mass flow reduces again as the resistance of the two-phase flow in the riser increases with increasing void fraction.

The simulations presented here used the Müller-Steinhagen and Heck correlation function to determine the pressure drop of the flow. This correlation function produces the smallest pressure drop for two-phase flow. If a different correlation function is used, the

Table 5
Design data ILL Helium Loop.

Name	Buffer	Line	Supply	HX	Retour	Cooler	Unit
Material	SS304	SS304	SS304	Al6061	SS304	Al6061	–
ϵ_c	0.1	0.1	0.05	0.1	0.05	0.1	–
h_e	1000	1	0.001	0.001	0.001	0.1	W/m ² /K
d_w	1	2	2	2	2	2	mm
T_e	300	300	300	300	300	300	K
D	20	35.5	60	20	60	20	mm
ϵ	10	10	10	10	10	10	ppm
ΔH	0	5	–1	1	0	0	m
ΔL	1	10	27	1	27	0.5	m
A_C	1					1	m ²
V_C	0.92					0.15	m ³

Table 6
Volumes and masses ILL Mockup Loops.

Name	Volume dm ³	Area m ²	Content mass gram	Empty mass kg
Moderator Cell	7	0.132	1050	0.358
Heat exchanger	19	30.2	639	54
CNSBuffer	4000	8	969	640
Cold CNS Loop	32.65	31.4	2281	57.5
Total CNS Loop	4039	40.6	3252	716
Cooler	150	1	1294.6	5.4
HXShellSide	6	30.2	38.9	8.2
CoolerBuffer	920	1	473.0	80
Cold Cooler Loop	308.7	41.34	2428	176
Total Cooler Loop	1239	43.45	2960	274

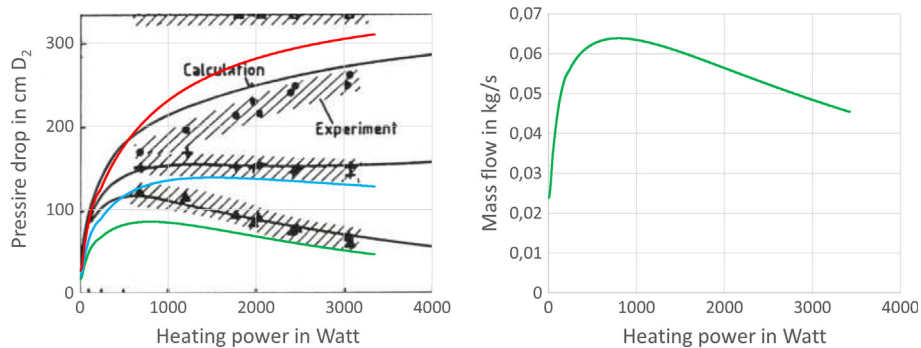


Fig. 6. Flow pressure drops (left side) and mass flow (right side) as function of applied heat load for ILL deuterium Mockup loop. The background of the graph was taken from Hoffmann [17]. The black dots and hatched areas represent the measurements and estimated accuracy region of pressure drops in the loop. The black lines represent calculations as presented by Hoffmann. The colored lines represent the same pressure drops calculated using the simulations as presented here. Lower (green) line: pressure drop over downcomer, middle (blue) line: pressure drop over downcomer and moderator cell, upper (red) line: pressure drop over downcomer, moderator cell and riser. (For interpretation of the references to colour in this figure legend, the reader is referred to the web version of this article.)

maximum flow shifts to smaller heating powers. The differences between Müller-Steinhagen-Heck and Friedel correlations are small (less than 15%) and the differences between Chisholm and Lockhart-Martinelli correlations are also small (less than 20%), but the latter pair deviate more from the experimental values than the former pair.

Fig. 7 shows the corresponding development of the void fraction in the moderator cell. This curve strongly depends on initial void fraction and other parameters. The slope is 7.8%/kW. It is possible to increase the void fraction entering the downcomer from 0 (single phase as in the above calculations) to 0.15...0.5 (the maximum depending on the liquid contents of the heat exchanger, hence of the applied heat load). Because of the higher void fraction in the downcomer the pressure head (determined by the difference in weight of the riser and downcomer) is reduced and the mass flow is reduced so that the total pressure drop due to flow friction

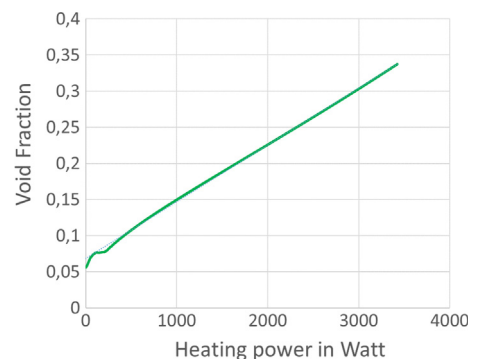


Fig. 7. Void fraction as function of applied heat load for ILL deuterium Mockup loop.

is less. The behavior of the loop is strongly dependent on the actual void fraction entering the downcomer. The agreement with the measurement is worse than in the previous case, and the maximum in mass flow occurs for much larger heating powers. The resulting void fraction in the moderator cell is significantly higher, but less sensitive to the actual heat load on the moderator cell (the slope reduces from 7.8%/kW to 5.8%/kW).

5. Conclusions

With the method described here it is possible to simulate a thermosyphon loop and determine the order of magnitude of the relevant time constants and the typical behavior of the flow. The method is successfully applied to two cryogenic thermosyphon loops in use for the cooling of cold neutron sources. It can be used to study the void fraction in the moderator cell and yields valuable information on the performance of a particular design. Accurate simulations can be done if more data about the process conditions (like temperature, pressure, flow rate) for changing experimental conditions (like for instance total mass of the loop, length and diameter of pipes) are available. Then also the influence of changing design parameters can be studied.

Appendix A. Void fraction moderator cell

Void fraction is defined as the relative amount of gas inside the liquid moderator. The gas is created by boiling of the liquid moderator. The boiling is due to the heat load on the moderator liquid and moderator containment. The heat load is partly produced by the nuclear heating due to neutron and gamma absorption, partly by heat radiation and partly by conduction.

Due to its shape, the moderator cell cross section from bottom to top is first increased and then decreased. This means that the velocity of the flow first decreases and then increases again. The complete flow pattern is complicated and different when details in the moderator cell change. Hence, it is impossible to accurately determine the void fraction of the moderator cell with this method.

The liquid will enter the cell at the bottom and exit at the top (as is sensible for a boiling source). Almost no liquid will go up the riser until the level of the liquid plus bubbles rising from the hot surfaces of the moderator cell is such that the space above the liquid is a froth, at which point the froth will exit the vessel with entrained liquid. This is in fact obvious from a consideration of the flow and boiling process. There is no mechanism to entrain any significant amount of liquid in the flow. The actual volumetric vapor flow is low (heat input less than the critical boiling limit), so we have pool boiling. It is only when the cell filling (by the total volume of liquid plus bubbles) results in an overflow condition that the liquid is swept into the riser, where the velocity is high enough to support liquid transport.

Here, the condition that no liquid leaves the cell until the total volume of liquid in the cell has reached a certain volume is imposed. When the amount of liquid becomes larger, the vapor quality exiting the cell is taken in relation to the remaining volume according to a cosine profile (starting with 1 and ending with 0 when the cell is completely filled). The volume when the vapor quality in the riser starts to decrease from 1 is called the *overflow volume*, V_o and can be estimated by means of pool boiling calculations, by CFD simulations using the geometry of the cell, or by actual measurement.

Appendix B. Hydrogen condensation in heat exchanger

Inside the tubes vapor (temperature T) condenses releasing its heat to the inner tube wall (temperature T_i) and forms a conden-

sate film (thickness d) that starts flowing downwards due to gravity (gravity constant g). During its fall downwards more vapor is condensed so that the film thickness increases. Hence the film thickness and the heat transfer coefficient changes. According to Nusselt [18] the film thickness as function of the film length, z is given by

$$d(z) = \left[\frac{4z(T - T_i)}{g} \frac{\lambda^L \eta^L}{\rho^L(\rho^L - \rho^V)H} \right]^{\frac{1}{4}} \quad (\text{B.1})$$

and the heat transfer coefficient by

$$h(z) = \left[\frac{g}{4z(T - T_i)} \frac{(\lambda^L)^3 \rho^L(\rho^L - \rho^V)H}{\eta^L} \right]^{\frac{1}{4}} \quad (\text{B.2})$$

where the material properties are taken for the average film temperature that can best be taken as $(2T_i + T)/3$, λ^L is the heat conductivity of the liquid at this temperature, ρ^L is the density of the liquid, ρ^V the density of the vapor, η^L is the dynamic viscosity of the liquid and H the heat released during condensation. In principle these equations only hold for small film Reynolds numbers (<30) defined as

$$Re_f(z) = \frac{4\rho^L v(z)d(z)}{\eta^L} \quad (\text{B.3})$$

where $v(z)$ is the average velocity of the liquid in the film. However, when the Reynold number increases the heat transfer coefficient is in general higher, so that this value is conservative for calculating the temperature difference [4]. When averaged over the length, L of the tubes, the heat transfer coefficient is given by

$$h_a(L) = \frac{4}{3} h(L). \quad (\text{B.4})$$

Now the heat transfer due to condensation can be expressed as

$$Q = nh_a \pi D_i L (T - T_i) \quad (\text{B.5})$$

where n is the number of tubes and D_i their inner diameter.

Due to its shape, the complete flow pattern in the heat exchanger is complicated and different when details change. Hence, it is impossible to determine the void fraction of the heat exchanger with this method accurately. The condensed liquid will flow in the volume at the bottom of the heat exchanger and almost no liquid will go down the downcomer until the level of the liquid is such that it can spill into the downcomer. The spill will eventually give rise to a vapor quality of 0 of the flow into the downcomer when the spill is large enough and the entrance of the downcomer has been designed properly.

Here, the condition that no liquid leaves the heat exchanger until the total volume of liquid in the heat exchanger has reached a certain volume is imposed. When this volume this is reached the vapor quality exiting the heat exchanger is taken in relation to the remaining spill volume according to a cosine profile (starting with 0 and ending with 1 when the remaining spill volume is completely filled). The volume when the vapor quality in the downcomer starts to decrease from 1 is called the *overflow volume*, V_o and must be determined by means of CFD simulations using the geometry of the heat exchanger or by actual measurement. The same holds for the remaining spill volume (determined by a factor σ_o times the overflow volume) after which the vapor quality is 0 and the downcomer is completely filled with liquid.

Appendix C. Heat conduction through container wall

The heat released to the container walls by condensation, convection or radiation is transported to the cold side of the container walls by means of conduction and is used to heat up or cool down

the container wall. The temperature, T in the wall as function of location, x and time, t can be found by solving Fourier's Law

$$\frac{\partial T}{\partial t} = a \frac{\partial^2 T}{\partial x^2} \quad (\text{C.1})$$

where $a = \lambda / \rho C_p$ is the thermal diffusivity, with λ the thermal conductivity of the wall material, ρ its density and C_p its heat capacity. The general solution of the above equation is

$$T(x, t) = \int \left\{ A(\kappa) \sin \frac{\kappa x}{d} + B(\kappa) \cos \frac{\kappa x}{d} \right\} e^{-t\kappa^2/\tau} d\kappa \quad (\text{C.2})$$

where $\tau = d^2/a$. For a metal wall of 1 mm thickness this time constant is of the order of 1 s. A specific solution for long times is given by

$$T(x, t) = T_o + T_1 \frac{x}{d} + \left\{ A \sin \frac{\kappa x}{d} + B \cos \frac{\kappa x}{d} \right\} e^{-t\kappa^2/\tau}. \quad (\text{C.3})$$

For all t , for $x = 0$ (inner side of the wall) the heat flux is given by

$$\frac{Q}{A_c} + P^S + P^W d\rho = \lambda \frac{\partial T}{\partial x} \Big|_{x=0} \quad (\text{C.4})$$

where

$$\frac{Q}{A_c} = h_c(T(0, t) - T) \quad (\text{C.5})$$

is the heat flux towards the content due to the temperature difference between contents and wall, P^S is the additional heat load (or sink when <0) on the inner side of the wall, P^W is the nuclear heat load density on the container wall. Hence, it is assumed that nuclear heating on the wall and the additional heat load act as constant fluxes from the inner side of the wall. This is not completely true, but because of the high conductivity of the wall this is a valid approximation.

For all t , for $x = d$ (outer side of the wall) the heat flux is given by

$$\frac{Q^R + Q^C}{A_c} = \lambda \frac{\partial T}{\partial x} \Big|_{x=d}. \quad (\text{C.6})$$

Further,

$$Q^C = A_c h_e (T_e - T(d, t)) \quad (\text{C.7})$$

where $T(d, t)$ is the outside temperature of the container wall, T_e is the environmental temperature, A_c is the effective area of the container and h_e is the heat transfer coefficient of the container to the environment and the radiation heat flow is proportional to the 4th power of the temperatures

$$Q^R = A_c \epsilon_c \sigma_B (T_e^4 - \{T(d, t)\}^4) \quad (\text{C.8})$$

where $\sigma_B = 5.67 \times 10^{-8} \text{ W}/(\text{m}^2 \text{ K}^4)$ is Stephan-Boltzmann's constant and ϵ_c is the emissivity coefficient. This can be written as

$$Q^R = A_c h_R (T_e - T(d, t)) \quad (\text{C.9})$$

where

$$h_R = \epsilon_c \sigma_B (T_e^2 + T(d, t)^2) (T_e + T(d, t)) \quad (\text{C.10})$$

so that

$$\frac{Q^R + Q^C}{A_c} = (h_R + h_e)(T_e - T(d, t)) = \lambda \frac{\partial T}{\partial x} \Big|_{x=d}. \quad (\text{C.11})$$

The solution reads

$$T_1 = \frac{T_e - T + \frac{P^S + P^W d\rho}{h_c}}{1 + \frac{\mu_e + \mu_c}{\mu_e \mu_c}}, \quad T_o = T_e - T_1 \left(1 + \frac{1}{\mu_e}\right), \quad (\text{C.12})$$

$$B = T(0, 0) - T_o, \quad A = \frac{\mu_c}{\kappa} B,$$

where $\mu_e = dh_e/\lambda$ is the Biot number for the heat resistance at the outside wall. A low Biot number means that the heat resistance is mainly at the outside of the wall and not due to conduction in the wall. Here the Biot number at the outer side of the wall is always small. $\mu_c = dh_c/\lambda$ is the Biot number for the heat resistance at the inner side of the wall. This depends on the flow rate, temperature and density. κ should be a solution of

$$\tan \kappa = \frac{\kappa(\mu_e + \mu_c)}{\kappa^2 - \mu_e \mu_c}. \quad (\text{C.13})$$

The smallest possible absolute value of κ should be used. Hence $\kappa > \sqrt{\mu_e \mu_c}$. The solution can be rewritten as

$$T(x, t) = T_o + T_1 \frac{x}{d} + (T(0, 0) - T_o) \left\{ \frac{\mu_c}{\kappa} \sin \frac{\kappa x}{d} + \cos \frac{\kappa x}{d} \right\} e^{-t\kappa^2/\tau}. \quad (\text{C.14})$$

Appendix D. Temperature increase of the container contents

D.1. All vapor content

The heat released from the container walls, Q , the nuclear heating of the contents, P and the mass flow through the container will change the temperature according to

$$mC_p \frac{\partial T}{\partial t} = Q + Q_f + mP \quad (\text{D.1})$$

where m is the mass of the contents, C_p is the heat capacity at constant pressure, T is the temperature of the contents and t represents time. As before $Q = A_c h_c (T_i - T)$, where A_c is the container surface area and h_c the heat transfer coefficient between container wall (at temperature T_i) and content. Q_f occurs because the enthalpy of the mass flow entering the container is different from the enthalpy leaving the container, according to

$$Q_f = \Phi_e^L H_e^L + \Phi_e^V H_e^V - (\Phi^L H^L + \Phi^V H^V)$$

where Φ_e^L is the liquid mass flow and H_e^L the enthalpy entering the container from the connected element and Φ_e^V and H_e^V the same for the gaseous or vapor phase. Φ^L is the liquid mass flow and H^L the enthalpy leaving the container and Φ^V and H^V the same for the gaseous or vapor phase. The above Eq. (D.1) can be rewritten as

$$\frac{\partial y}{\partial t} = \frac{P}{C_p} - \frac{y}{\tau} \quad (\text{D.2})$$

where $y = T - T_i - Q_f/(A_c h_c)$ and $\tau = mC_p/(A_c h_c)$. The general solution is

$$T(t) = T(0) + \left(T_i + \frac{Q_f + mP}{A_c h_c} - T(0) \right) (1 - e^{-t/\tau}). \quad (\text{D.3})$$

This solution will be followed as long as the temperature is above the saturation temperature, T_s of the contents at the specific density or pressure. In case the temperature would drop below this temperature, (if $T_i + (Q_f + mP)/(A_c h_c) < T_s$) the gas starts condensing at the saturation temperature. In that case first the time is calculated at which condensation will start

$$t_s = \tau \ln \frac{T(0) - T_i - (Q_f + mP)/(A_c h_c)}{T_s - T_i - (Q_f + mP)/(A_c h_c)} \quad (\text{D.4})$$

and during the remaining time, $t - t_s$, the gas will condense into liquid according to the next paragraph.

D.2. Vapor and liquid content

The heat released from the container walls, the nuclear heating of the contents and the mass flow through the container will change the vapor/liquid content according to

$$(m^L(t) - m^L(0))(H^L - H^V) = (A_c h_c (T_i - T) + Q_f + mP)t \quad (D.5)$$

where m is the total mass of the content, $m^L(t)$ is the liquid mass at time t . $H^L - H^V$ is the enthalpy difference between the liquid and vapor state of the contents at content temperature, T . A_c the container surface area, h_c the heat transfer coefficient between container wall (at temperature T_i) and content, P the nuclear heating of the contents. Note that the total mass of the content is fixed ($m^L(t) + m^V(t) = m$) and the heat load/sink is absorbed/released by evaporation/condensation of part of this mass.

This solution will be followed as long as there is a mixture of liquid and vapor. If the right hand side of the above equation is positive evaporation occurs, if it is negative condensation occurs. For condensation, the maximum time until single phase occurs is when $m^L(t) = m$

$$t_m = \frac{m^V(0)(H^L - H^V)}{A_c h_c (T_i - T) + Q_f + mP} \quad (D.6)$$

so that

$$m^L(t) = m^L(0) \left(1 - \frac{t}{t_m}\right) + m \frac{t}{t_m}, \quad (D.7)$$

$$m^V(t) = m^V(0) \left(1 - \frac{t}{t_m}\right) \quad (D.8)$$

or when $m^L(t) = 0$

$$t_m = -\frac{m^L(0)(H^L - H^V)}{A_c h_c (T_i - T) + Q_f + mP} \quad (D.9)$$

so that

$$m^L(t) = m^L(0) \left(1 - \frac{t}{t_m}\right), \quad (D.10)$$

$$m^V(t) = m^V(0) \left(1 - \frac{t}{t_m}\right) + m \frac{t}{t_m} \quad (D.11)$$

and during the remaining time, $t - t_m$, the gas will heat up according to the previous paragraph or the liquid will cool down according to the next paragraph.

D.3. All liquid content

The heat released from the container walls, the nuclear heating of the contents and the mass transport into the content will change the temperature similar to the first paragraph with the same general solution (D.3). This solution will be followed as long as the temperature is below the saturation temperature, T_s of the contents at the specific density or pressure. In case the temperature would rise above this temperature, (if $T_i + (Q_f + mP)/(A_c h_c) > T_s$) the liquid starts evaporating at the saturation temperature. In that case, first the time at which evaporation will start is calculated according to

$$t_s = \tau \ln \frac{T_i - T(0) + (Q_f + mP)/(A_c h_c)}{T_i - T_s + (Q_f + mP)/(A_c h_c)} \quad (D.12)$$

and during the remaining time, $t - t_s$, the gas will evaporate according to the previous paragraph.

Appendix E. Adiabatic mass transport to obtain new pressure equilibrium

The change in enthalpy during heating/cooling of the content will give rise to changing material properties, giving rise to a changing pressure distribution in the loop. To find the new pressure distribution, the pressure in the heat exchanger (or buffer) is first adapted and further the pressures in the complete loop, based on the required pressure differences due to the resistance of the mass flow. It is assumed that this distribution has occurred during the preceding time step and that it occurred adiabatically. The total mass in the system is constant so that one must keep track of where the mass of the content is going to and what energy transfer is related to that. This is done for each element.

Two situations can occur. First, if the final mass density, ρ in an element is less than its start mass density, ρ_o then the entropy change will be 0. This means that all mass leaving the content leaves with its start entropy density, S_o and for the rest of the contents no time is left to take up energy from surroundings. Second, if the final mass density in an element is larger than its start mass density the entropy change of the initial mass will be 0, but the entropy density, S_e of the additional mass is added. This means that the total entropy of all material is constant, as it must for ideal adiabatic expansion/compression.

Hence, the total relevant entropy at the start is

$$\rho_o S_o + (\rho - \rho_o) S_e u(\rho - \rho_o) \quad (E.1)$$

where $u(x)$ is the Heaviside step function ($u(x) = 0$ for $x < 0$ and $u(x) = 1$ for $x \geq 0$). The first term is the total entropy in the content, the second term is the entropy of the mass entering the content. The total relevant entropy at the end is

$$\rho S(\rho, T) + (\rho_o - \rho) S_o u(\rho_o - \rho). \quad (E.2)$$

The first term is the total entropy in the content, the second term is the entropy of the mass exiting the content. The change between start and end is adiabatic, hence the entropy does not change so that

$$\rho(S(\rho, T) - S_o) = (\rho - \rho_o)(S_e - S_o)u(\rho - \rho_o). \quad (E.3)$$

E.1. Single phase

For a single phase the entropy is a continuous function of the density and temperature. However, as the entropy change is realized at a final pressure, p the density and temperature are related to each other. Hence, the above equation has 1 unknown only and can be solved iteratively. In such a case the final density can only be larger than the initial density, if the final pressure is larger than the initial pressure, then $u(\rho - \rho_o) = 1$ and

$$\rho = \rho_o \frac{S_o - S_e}{S(\rho, T(\rho, p)) - S_e}. \quad (E.4)$$

In case the final pressure, p is smaller than the initial pressure, then the final density is smaller than the initial density so that $u(\rho - \rho_o) = 0$ and

$$S(\rho, T(\rho, p)) = S_o. \quad (E.5)$$

E.2. Two phases

Two phases can only occur when the temperature is at the saturation temperature at the final pressure, p . Then the entropy density of the liquid phase, S^L and the entropy density of the vapor phase, S^V are fixed as are the densities of the liquid, ρ_L and vapor ρ_V phase. In such a case a change in entropy is realized by either

condensation or evaporation. The average density of the content is defined as

$$\rho = \alpha\rho_v + (1 - \alpha)\rho_L \quad (\text{E.6})$$

where $\alpha\rho_v$ is the mass per volume of the vapor part and $(1 - \alpha)\rho_L$ is the mass per volume of the liquid part. The vapor quality, x is defined as the ratio between the mass of the vapor part and the total mass, hence

$$x = \frac{\alpha\rho_v}{\rho} = \frac{\rho_L - \rho}{\rho_L - \rho_v} \frac{\rho_v}{\rho} \quad (\text{E.7})$$

The average entropy density can be written as

$$S = xS^v + (1 - x)S^l \quad (\text{E.8})$$

so that the total entropy of the content at the end is

$$\rho S = \rho S^c + \rho_o S^o \quad (\text{E.9})$$

with

$$S^c = \frac{\rho_L S^l - \rho_v S^v}{\rho_L - \rho_v} \quad \text{and} \quad S^o = \frac{\rho_L \rho_v}{\rho_o(\rho_L - \rho_v)} (S^v - S^l). \quad (\text{E.10})$$

Note that S^c and S^o are material properties that only depend on the required pressure after the step. The change between start and end is adiabatic hence the entropy does not change

$$\rho S = \rho S_o + (\rho - \rho_o)(S_e - S_o)u(\rho - \rho_o) \quad (\text{E.11})$$

so that

$$\frac{\rho}{\rho_o} = \frac{S^o + (S_e - S_o)u(\rho - \rho_o)}{S_o - S^c + (S_e - S_o)u(\rho - \rho_o)} \quad (\text{E.12})$$

with a solution when $\rho < \rho_o$

$$\frac{\rho}{\rho_o} = \frac{S^o}{S_o - S^c} < 1. \quad (\text{E.13})$$

As $S^o > 0$ this occurs when $S_o > S^o + S^c$. When $\rho > \rho_o$ or $S_o < S^o + S^c$

$$\frac{\rho}{\rho_o} = \frac{S^o + S_e - S_o}{S_e - S^c} > 1 \quad (\text{E.14})$$

which has only a valid solution when $S_e > S^c$. The above solutions exist when also $\rho_v < \rho < \rho_L$, otherwise after the step the content will be single phase vapor ($\rho < \rho_v$) or single phase liquid ($\rho > \rho_L$).

Appendix F. Pressure drop calculations

F.1. Pure vapor flow

For pure vapor flow the liquid flow is absent and the total flow is considered single phase flow. In such a case the friction coefficient for a pipe is given by the Darcy friction factor. This is only dependent on Reynolds number and relative roughness of the surface. If $Re < 2100$:

$$f = \frac{64}{Re} \quad (\text{F.1})$$

otherwise:

$$f = \left\{ -2 \log \left[\frac{\epsilon}{3.71D} + \frac{2.18}{Re} \ln \frac{Re}{1.816 \ln \frac{1.1Re}{\ln(1+1.1Re)}} \right] \right\}^{-2} \quad (\text{F.2})$$

where ϵ is the surface roughness, D the effective diameter and Re is Reynolds number given by

$$Re = \frac{\rho_v v_v D}{\eta_v} = \frac{\phi_v D}{\eta_v A} \quad (\text{F.3})$$

where ρ_v is the vapor density, v_v is the vapor velocity, η_v is the vapor dynamic viscosity and A the effective area of the pipe cross

section. ϕ_v is the mass flow. The material properties depend on the temperature and pressure of the vapor. For smooth pipes the friction coefficient reduces to

$$f = \frac{64}{Re} \quad (\text{F.4})$$

if $Re < 2100$; otherwise:

$$f = \{0.79 \ln Re - 1.64\}^{-2}. \quad (\text{F.5})$$

The pressure difference per element length between element and input/output is given by

$$\frac{\Delta p}{\Delta L} = f \frac{\rho_v v_v^2}{2D} = f \frac{\phi_v^2}{2DA^2 \rho_v}. \quad (\text{F.6})$$

F.2. Pure liquid flow

For pure liquid flow the vapor flow is absent and the total flow is considered single phase flow. In such a case the friction coefficient for a pipe is given by the Darcy friction factor and the pressure difference per element length between element and input/output is given by the above Eq. (F.6), where instead of the vapor properties the liquid properties are taken.

F.3. Two-phase flow

The total pressure drop is given by the sum of the static pressure drop (i.e. due to the height difference), the momentum pressure drop (due to acceleration of the flow when it converts to gas or liquid) and the frictional pressure drop.

The static pressure drop is given by

$$\frac{\Delta p_s}{\Delta L} = \rho_{tp} g \sin \theta \quad (\text{F.7})$$

where g is the gravitational acceleration and θ is the angle of the container with respect to the horizontal. The two-phase density is given by [19]

$$\rho_{tp} = \rho_L(1 - \alpha) + \rho_v \alpha \quad (\text{F.8})$$

where the void fraction is determined from the vapor quality, x according to

$$\alpha = \frac{x}{\rho_v} \left[C_o \left(\frac{x}{\rho_v} + \frac{1 - x}{\rho_L} \right) + \frac{U_G A}{\phi} \right]^{-1} \quad (\text{F.9})$$

with

$$C_o = 1 + 0.2(1 - x) \left(\frac{gD\rho_L^2 A^2}{\phi^2} \right)^{0.25}$$

and

$$U_G = 1.18 \left[\frac{g\sigma}{\rho_L} \left(1 - \frac{\rho_v}{\rho_L} \right) \right]^{0.25}$$

where σ is the surface tension of the liquid. This holds for vertical up flow. For vertical down flow the sign of U_G is changed.

The momentum pressure difference per element length between input and output is given by [19]

$$\frac{\Delta p_{mom}}{\Delta L} = \frac{\Delta(\phi^2 / (A^2 \rho_{tp}))}{\Delta L} = f_{mom} \frac{\phi^2}{2DA^2 \rho_v} \quad (\text{F.10})$$

where

$$f_{mom} = \frac{2D}{\Delta L} \left\{ (\rho_v / \rho_{tp})_{out} - (\rho_v / \rho_{tp})_{in} \right\}$$

so that $|f_{mom}| < \frac{2D}{\Delta L}$ as $\rho_V \leq \rho_{tp} \leq \rho_L$. So, the maximum momentum pressure drop corresponds to a friction factor of $2D/\Delta L$ where D is the diameter of the element and ΔL its length when the vapor quality changes from 0 to 1. A high heat input is needed to change the vapor quality so drastically. The heat input is mainly applied to the moderator cell, while in the rest of the loop the heat input is relatively small. Hence, the momentum pressure drop (and the influence of the heat input on the friction pressure drop in the elements) can be ignored. These are only relevant for the moderator cell, where the ratio of $2D/\Delta L$ is of the order of 1, comparable to the friction factor of the inlet or outlet of the cell. The flow resistance (be it frictional or momentum transfer) of the moderator cell is very hard to predict analytically and here a practical model has been assumed as described in Appendix A.

The frictional pressure drop can be calculated using the Friedel correlation model [19] applied to two-phase flow through a pipe. The frictional pressure difference per element length between element and input/output is given by

$$\frac{\Delta p}{\Delta L} = f \frac{\rho_V v_V^2}{2D} = \Phi_{fr} f_L \frac{\phi^2}{2DA^2 \rho_L} \quad (F.11)$$

where the Darcy friction factor f_L is determined as before by using the Reynolds number

$$Re_L = \frac{D\phi}{\eta_L A} \quad (F.12)$$

with the two-phase multiplier given by

$$\Phi_{fr} = E + \frac{3.24FH}{Fr^{0.045} We^{0.035}} \quad (F.13)$$

where

$$E = (1-x)^2 + x^2 \frac{\rho_L f_V}{\rho_V f_L} \quad (F.14)$$

$$F = x^{0.78} + (1-x)^{0.224} \quad (F.15)$$

$$H = \left(\frac{\rho_L}{\rho_V}\right)^{0.91} \left(\frac{\eta_V}{\eta_L}\right)^{0.19} \left(1 - \frac{\eta_V}{\eta_L}\right)^{0.7} \quad (F.16)$$

$$Fr = \frac{1}{gD\rho_H^2} \left(\frac{\phi}{A}\right)^2 \quad (F.17)$$

$$We = \frac{D}{\sigma\rho_H} \left(\frac{\phi}{A}\right)^2 \quad (F.18)$$

and

$$\rho_H = \left(\frac{x}{\rho_V} + \frac{1-x}{\rho_L}\right)^{-1} \quad (F.19)$$

The Darcy friction factor f_V is determined as before by using the Reynolds number

$$Re_V = \frac{D\phi}{\eta_V A} \quad (F.20)$$

In case of Müller-Steinhagen and Heck correlation the two-phase multiplier is defined as

$$\Phi_{MSH} = \left\{ 1 + 2x \left(\frac{\rho_L f_V}{\rho_V f_L} - 1 \right) \right\} (1-x)^{1/3} + \frac{\rho_L f_V}{\rho_V f_L} x^3 \quad (F.21)$$

and for the Chisholm correlation

$$\Phi_{CH} = 1 + \left(\frac{\rho_L f_V}{\rho_V f_L} - 1 \right) \left\{ B \left(\frac{\Phi}{A\Psi_o}, \sqrt{\frac{\rho_L f_V}{\rho_V f_L}} \right) x^{0.875} (1-x)^{0.875} + x^{1.75} \right\} \quad (F.22)$$

where $\Psi_o = 500 \text{ kg/m}^2\text{s}$ and $B(z_1, z_2)$ is given by

$$\begin{aligned} 0 < z_2 < 9.5 \quad z_1 > 3.8 & \frac{4.8}{\sqrt{3.8z_1}} \\ 1 < z_1 \leq 3.8 & \frac{4.8}{z_1} \\ z_1 \leq 1 & 4.8 \\ 9.5 < z_2 < 28 \quad z_1 \leq 1.2 & \frac{23.4}{z_2 \sqrt{z_1}}, \\ z_1 > 1.2 & \frac{23.4}{z_2 \sqrt{1.2}} \\ z_2 > 28 \quad z_1 \leq 1.2 & \frac{598}{z_2^2 \sqrt{z_1}} \\ z_1 > 1.2 & \frac{598}{z_2^2 \sqrt{1.2}} \end{aligned} \quad (F.23)$$

and for the Lockhart-Martinelli correlation

$$\Phi_{LM} = (1 + CX_{tt} + X_{tt}^2)(1-x)^2 \frac{f((1-x)Re_L)}{f(Re_L)} \quad (F.24)$$

where $X_{tt} = (x/(1-x))^{0.9} (\rho_L/\rho_V)^{0.5} (\eta_L/\eta_V)^{0.1}$, $f(Re)$ is the friction factor corresponding to Reynolds number Re and C is given by

$$\begin{aligned} (1-x)Re_L > 2300 \quad xRe_V > 2300 \quad C = 20 \\ xRe_V \leq 2300 \quad C = 10 \\ (1-x)Re_L \leq 2300 \quad xRe_V > 2300 \quad C = 12 \\ xRe_V \leq 2300 \quad C = 5 \end{aligned} \quad (F.25)$$

In case of two-phase hydrogen flow of 3 g/s at 23 K, Müller-Steinhagen and Heck correlation gives the smallest two-phase multiplier, then Friedel, Chisholm and Lockhart-Martinelli.

For the two-phase heat transfer coefficient we use

$$h_{tp} = h_L(1-\alpha) + h_V\alpha \quad (F.26)$$

$$h_L = \frac{\lambda_L Nu_L}{D} \quad \text{and} \quad h_V = \frac{\lambda_V Nu_V}{D} \quad (F.27)$$

where Nu_L and Nu_V are determined by using the Dittus-Boelter relation with Re_L, Pr_L and Re_V, Pr_V respectively.

References

- [1] European Spallation Source; 2016. <<https://europenspallationsource.se/european-spallation-source>>.
- [2] OYSTER; 2016. <<http://www.tnw.tudelft.nl/en/cooperation/facilities/reactor-instituut-delft/oyster/>>.
- [3] Dobson RT, Ruppertsberg JC. Flow and heat transfer in a closed loop thermosyphon. Part I - theoretical simulation. J Energy Southern Africa 2007;3:32–40.
- [4] Dobson RT. Relative thermal performance of supercritical co2, h2o, n2, and he charged closed-loop thermosyphontype heat pipes. Heat Pipe Sci Technol Int J 2012;3(2–4):169–85.
- [5] Kaya T, Pérez R, Gregori C, orres A. Numerical simulation of transient operation of loop heat pipes. Appl Therm Eng 2008;28:967–74.
- [6] Bieliński H, Mikieliewicz J. Natural circulation in single and two phase thermosyphon loop with conventional tubes and minichannels. IntechOpen; 2011.
- [7] Zhang P, Li X, Shang S, Shi W, Wang B. Effect of height difference on the performance of two-phase thermosyphon loop used in air-conditioning system. In: 15th International refrigeration and air conditioning conference at Purdue, July 14–17 2014.
- [8] McAdams WH. Heat transmission. 2nd ed. New York: McGraw-Hill; 1942.
- [9] Leachman JW, Jacobsen RT, Penoncwello SG, Lemmon EW. Fundamental equations of state for parahydrogen, normal hydrogen, and orthohydrogen. J Phys Chem Ref Data 2009;38:721–48.
- [10] Assael MJ, Assael J-AM, Huber ML, Perkins RA, Takata Y. Correlation of the thermal conductivity of normal and parahydrogen from the triple point to 1000 K and up to 100 MPa. J Phys Chem Ref Data 2011;40. 033101–1:13.
- [11] Muzny CD, Huber ML, Kazakov AF. Correlation for the viscosity of normal hydrogen obtained from symbolic regression. J Chem Eng Data 2013;58:969–79.
- [12] Richardson IA, Leachman JW, Lemmon EW. Fundamental equation of state for deuterium. J Phys Chem Ref Data 2014;43(1).

- [13] Lemmon EW, Huber ML, McLinden MO. NIST standard reference database 23: reference fluid thermodynamic and transport properties-REFPROP, Version 9.1. Gaithersburg: National Institute of Standards and Technology, Standard Reference Data Program; 2013.
- [14] Bell Ian H, Wronski Jorrit, Quoilin Sylvain, Lemort Vincent. Pure and pseudo-pure fluid thermophysical property evaluation and the open-source thermophysical property library coolprop. *Ind Eng Chem Res* 2014;53(6):2498–508. PMID: 24623957.
- [15] Duthil P. Material properties at low temperature. ArXiv e-prints, January 2015.
- [16] Rowe JM. Analysis of bt-9 thermosiphon performance. *Int Rep* 2012.
- [17] Hoffmann H. Experimental investigations of the heat transfer behavior of a horizontally arranged cylindrical cold neutron source in a vaporizing deuterium flow. In: Collan H, Berglund P, Krusius M, editors. *Proc. of the 10th internat.cryogenic engineering conf.* Butterworth; 1984. p. 390–3.
- [18] Nusselt W. Die oberflächenkondensation des wasserdampfes. *Z Vereines Deutch Ing* 1916;60:541–6.
- [19] Thome JR. *Engineering data book III.* Germany: Wieland-Werke; 2014.